

PAPER

## Water contact angles on charged surfaces in aerosols

To cite this article: Yu-Tian Shen *et al* 2022 *Chinese Phys. B* **31** 056801

View the [article online](#) for updates and enhancements.

### You may also like

- [Electrical cycle in the Earth's atmosphere](#)  
B M Smirnov
- [Contribution of natural and anthropogenic aerosols to optical properties and radiative effects over an urban location](#)  
S Ramachandran, R Srivastava, Sumita Kedia *et al.*
- [Electrowetting on 2D dielectrics: a quantum molecular dynamics investigation](#)  
Jian Liu and Sokrates T Pantelides

# Water contact angles on charged surfaces in aerosols

Yu-Tian Shen(申钰田)<sup>1,2</sup>, Ting Lin(林挺)<sup>2</sup>, Zhen-Ze Yang(杨镇泽)<sup>2</sup>, Yong-Feng Huang(黄永峰)<sup>1,2</sup>,  
 Ji-Yu Xu(徐纪玉)<sup>1,2</sup>, and Sheng Meng(孟胜)<sup>1,2,†</sup>

<sup>1</sup>*Institute of Physics, Chinese Academy of Sciences, Beijing 100190, China*

<sup>2</sup>*University of Chinese Academy of Sciences, Beijing 100049, China*

(Received 2 December 2021; revised manuscript received 28 February 2022; accepted manuscript online 10 March 2022)

Interactions between water and solid substrates are of fundamental importance to various processes in nature and industry. Electric control is widely used to modify interfacial water, where the influence of surface charges is inevitable. Here we obtain positively and negatively charged surfaces using LiTaO<sub>3</sub> crystals and observe that a large net surface charge up to 0.1 C/m<sup>2</sup> can nominally change the contact angles of pure water droplets comparing to the same uncharged surface. However, even a small amount of surface charge can efficiently increase the water contact angle in the presence of aerosols. Our results indicate that such surface charges can hardly affect the structure of interfacial water molecular layers and the morphology of the macroscopic droplet, while adsorption of a small amount of organic contaminants from aerosols with the help of Coulomb attraction can notably decrease the wettability of solid surface. Our results not only provide a fundamental understanding of the interactions between charged surfaces and water, but also help to develop new techniques on electric control of wettability and microfluidics in real aerosol environments.

**Keywords:** water contact angle, charged surface, aerosols

**PACS:** 68.08.Bc, 68.08.–p

**DOI:** 10.1088/1674-1056/ac5c2f

## 1. Introduction

Interactions between water or aqueous solutions and solid substrates are fundamental to understand various physics, chemistry, and biological processes. Macroscopically, the interaction can be represented by wettability of solids or contact angle of droplet. Factors influence wettability of solids include chemical properties, nanostructures, cleanness, and electric controls, providing various prospects to understand and modify the interaction. Microscopically, hydrogen bonds and structures of highly polar water molecules on solids have been intensively studied. Understanding how the microscopic interactions would affect the macroscopic wettability is crucial in manipulation of liquid–solid interactions.

Owing to the advantages of easy operation and electrical reversibility, electric modification of the interaction between water and solid has been widely studied. Water freezes differently on positively or negatively charged surfaces of pyroelectric materials.<sup>[1]</sup> Electric field can control evaporation of aqueous droplets and suppress the coffee stain effect.<sup>[2]</sup> A small amount of charges can efficiently impact surface frictions between solids and water droplets.<sup>[3]</sup> The voltage applied can control the shapes of electrolyte solution droplets on solids in various ways as named electrowetting.<sup>[4–6]</sup> There are many studies on how surface charge or polarity affects aqueous wettability based on molecular dynamic simulations.<sup>[7–11]</sup> However, how the net surface charge affects the contact angle of water droplet has not yet been experimentally studied, let alone considering the participation of inevitable aerosol environments since the net-charged surface cannot be stable.

Here we obtain the net-charged surfaces using pyroelectric LiTaO<sub>3</sub> crystals and observe that the net surface charge up to 0.1 C/m<sup>2</sup> can nominally affect contact angles of pure water droplets compared to the neutral surface. However, if exposed in aerosols, even a small amount of organic contaminants can efficiently increase the contact angles of water droplets. Our experimental results contribute a fundamental understanding on the interaction between the charged surface and water, and is helpful for developing new ways of electric control of wettability and microfluidics in real aerosol environments.

## 2. Methods

Water contact angles are measured using dataphysics OCA20 and analyzed using software SCA20.U. We deposit water droplets on to *z*-cut LiTaO<sub>3</sub> crystals supported by an insulating holder in controlled aerosols and then take videos (Fig. 1(a)). The interval between adjacent frames is 34 ms. The deposition starts at the moment when the crystal is put onto the holder, and finishes within a minute to get surface charges according to the temperature difference. The value of contact angle is obtained from the first frame when the spherical cap droplet appears on the crystal to avoid the effect of evaporation on the shape of the water droplets. Water used is ultrapure water and the volume of every droplet is 0.5 ml. The *z*-cut LiTaO<sub>3</sub> crystals are purchased from Shanghai Institute of Optics and Fine Mechanics, Chinese Academy of Sciences. Since the wettability of surface is sensitive to its roughness,<sup>[12]</sup> we use +*z* surfaces of half of crystals to generate negative charges and –*z* surfaces of the other half for

<sup>†</sup>Corresponding author. E-mail: smeng@iphy.ac.cn

positive charges to avoid the abrasion which happens between the bottom surfaces of the crystals and the holder.

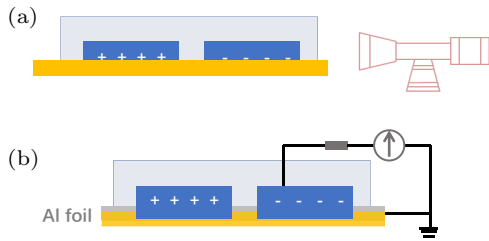


**Fig. 1.** Schematic for measuring contact angle and surface charge density on the variable temperature holder (yellow). (a) Measuring contact angle by taking sideview video, where water droplets (gray) are deposited on *z*-cut LiTaO<sub>3</sub> crystals (deep blue) in controlled aerosols (light blue). (b) Measuring surface charge density using an oscilloscope, where the crystals are placed on earthing aluminum foil (gray).

The value of the surface charge density is determined by the pyroelectric coefficient and temperature difference. The evolution of the surface charge density is presented by the detected evolution of the voltage generated at the surface in the controlled aerosols. Crystals are put on the holder covered by earthing aluminum foil and the discharging processes of the upper surfaces are detected by an oscilloscope (Fig. 1(b)). The voltage at the surface can be calculated using the peak of the voltage read in oscilloscope and the resistance of probes. The resistance of the oscilloscope and two probes is 1 M $\Omega$ , 10 M $\Omega$  and 60 M $\Omega$ , respectively.

The surface charge is controlled via abrupt temperature changes. For neutral surfaces at room temperature, the holder keeps room temperature. For neutral cases at other temperatures, the crystals are preheated in a thermostat water base of the same temperature of the holder. Wet crystals are put onto the holder and the evaporating water can bring away possible surface charges. For cases with surface charges, the charge density is controlled by transferring crystal at room temperature onto the heated holder. The crystal is dried by high purity nitrogen before transfer and every water droplet is deposited on a new place. The transferring process of each crystal is less than 40 seconds. The temperature of the holder is set from 30 °C to 70 °C, during which the density of surface charge is proportional to the temperature change since the pyroelectric coefficient of the LiTaO<sub>3</sub> crystal is constant.<sup>[13]</sup>

The crystals are rinsed by deionized water followed by two cycles of ultrasonic cleaning immersed in acetone-isopropyl alcohol–ethanol–ultra pure water. The span in each liquid is 5 min. We use UVO (ultra-violet ozone) treatment to clean crystals on which  $\cos(\theta)$  of water droplets is still lower than 0.85 after the ultrasonic cleaning. The adsorbed contaminations on the crystal surface depend on all environmental histories the crystal has ever experienced, which contain complex components and cannot be precisely controlled due to the complexity. The adsorption affects surface tension of the crystal, therefore the value of  $\cos(\theta)$  cannot be precisely controlled.<sup>[14–18]</sup> We finish collecting all data for the

same figure before detecting another one. Meanwhile, the error of  $\cos(\theta)$  is inevitable since the data in every figure contains many groups of data, of which the cleaning histories are not the same. The crystals are of the same cleaning history and exposure history in each group of data to guarantee that the tendency in each graph is comparable.

The temperature is controlled using the variable temperature holder dataphysics TPC 150. The crystal is put onto the holder of various temperatures. The duration of heat conduction is ignored since the thickness of the crystal is 0.5 mm and its thermal conductivity is about double of copper. The temperature of crystals becomes that of the holder before detections.

All detections take place in a semi-closed chamber on the holder. There is a slit (width, 2.0 mm) at the top of the chamber open to the air, through which the insulating syringe needle and the conducting probe come in. There is also a hole at the top of the chamber, through which high purity nitrogen flows from a pipe into the chamber. Three kinds of pipes are used, straight brass, straight teflon, and bent teflon. The bent teflon pipe is used unless otherwise stated. The straight pipes are 150 cm long and the bent one 190 cm long. The internal diameter of every pipe is 2.5 mm. The air of Beijing contributes to aerosols in the chamber, where the size of particulate matters mainly distributes in the range of 0.2–10  $\mu\text{m}$ .<sup>[19,20]</sup> The components are complex. A humidity probe in the chamber can monitor the relative humidity. Introducing high purity nitrogen can decrease the relative humidity in the chamber, thus control the aerosol inside. High purity nitrogen keeps flow into the chamber, except during the deposition of water droplet (within a minute) to prevent possible effects of gas flow on the shape of the droplet. The relative humidity is maintained to no more than 3 before measurements. Therefore, the effect of possible fluctuation of the air is limited in the chamber since the outside air is effectively diluted in the chamber.

The saturated vapor of 1-octadecene in Fig. 4(c) is obtained by placing liquid 1-octadecene in an open Petri dish in a closed chamber at room temperature. After an hour the crystals are put into the closed chamber for 50 min. 1-octadecene is only used in Fig. 4(c).

### 3. Obtaining charged surfaces using pyroelectric LiTaO<sub>3</sub>

To study how surface charges affect water contact angles, we should firstly obtain surfaces that can be artificially charged. We choose pyroelectric LiTaO<sub>3</sub> crystal, which is an insulator and can be charged on *z*-cut surfaces when the temperature changes. For pyroelectric crystals, its surface charge is the product of temperature change and pyroelectric coefficient. The pyroelectric coefficient of the LiTaO<sub>3</sub> crystal used here is  $2.3 \times 10^{-7} \text{ C}/(\text{cm}^2 \cdot \text{K})$ , which is constant below

100 °C.<sup>[13]</sup> Therefore, we can obtain opposite surface charges at opposite sides of the *z*-cut LiTaO<sub>3</sub> by controlling its temperature. When the temperature increases, one is negatively charged while the other is positively charged. When the temperature decreases, the surface charges are opposite. Since the duration of heat conduction is reasonably ignored (see methods), we assume that the temperature of the crystal becomes the temperature of the holder before detections.

We heat crystals from room temperature (RT). The maximum final temperature is 70 °C, corresponding to the surface charge density as high as 0.1 C/m<sup>2</sup>. The electric field strength is up to 0.02 V/Å in the crystal. We change the temperature no more than 50 °C to avoid the possibility that the aerosol environment could be broken through since electric fields are not perfectly confined inside the crystal. We detect the sur-

face charge density via voltage (see methods), which is proportional to the temperature change (Fig. 2(a)).

After the temperature changes, the charged surface cannot permanently sustain due to its interaction with environments.<sup>[1,21,22]</sup> The adsorption from the aerosol gradually neutralize it. The adsorption from the environment is inevitable even after neutralization. The surface charge is temporary when the charge equilibrium of the crystal and the environment is broken down. In the controlled aerosol (see methods), we detect the evolutions of the surface charge densities represented by the voltages for the duration of 60 min, as shown in Figs. 2(b)–2(d) (the voltages at 0 min are those in Fig. 2(a)). The surface charge density decreases at a higher rate when the final temperature is higher.

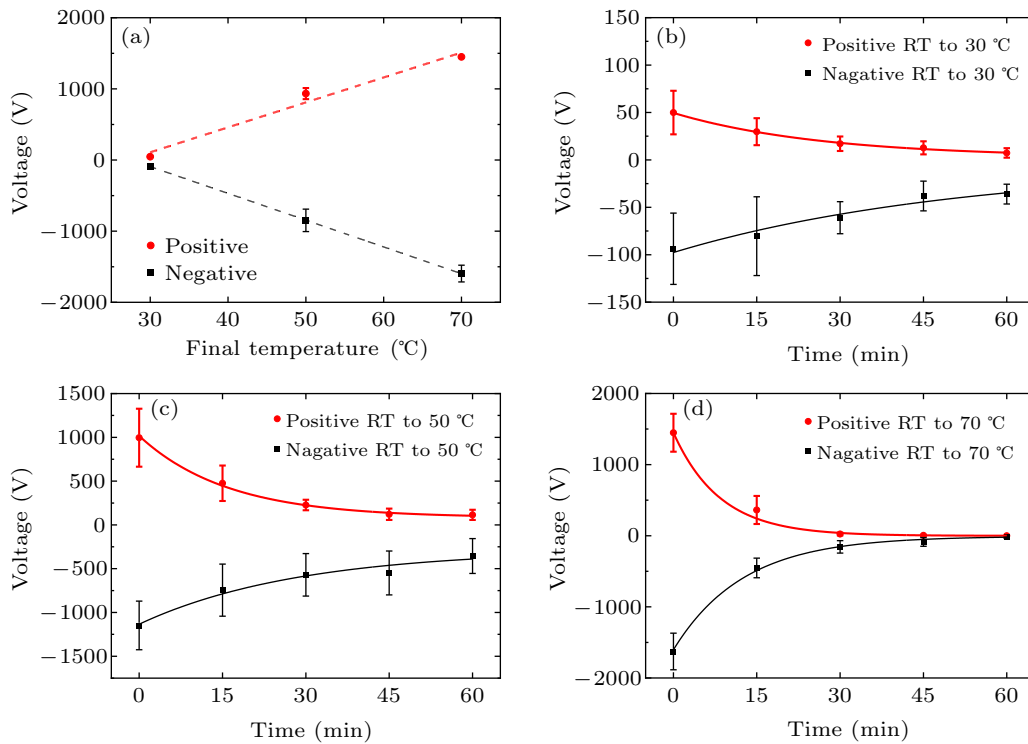


**Fig. 2.** Voltage generated as an indicator of surface charge density when LiTaO<sub>3</sub> crystals are heated from room temperature (RT) to various final temperatures. (a) Initial voltages at various final temperatures. Evolution of voltage in the controlled aerosol when the crystals are heated to (b) 30 °C, (c) 50 °C or (d) 70 °C.

#### 4. Water contact angle on charged surfaces

We deposited water droplets onto the charged surfaces in the controlled aerosol and detected the corresponding contact angles  $\theta$  (Fig. 3(a)). In comparison, WCA on the same surfaces without net charges is also measured as in Fig. 3(b), where ‘no positive’ or ‘no negative’ means the surfaces used to generate positive or negative charges in neutralized situations. The error is inevitably big since each figure contains dozens of times of cleaning with various surface tensions. However, in each group of data the crystals are of the same cleaning history, thus the tendency is comparable (more details see methods). Each measurement is finished within 1 min and the outside air is effectively diluted in the chamber (see the discussions on

Fig. 4(a)), thus the effect of possible fluctuation of the air on WCA is very limited.

On neutralized surfaces,  $\cos(\theta)$  keeps almost the same value at different temperatures with the deviation lower than 0.03. This ensures that the surfaces used to hold positive or negative charges are of the same wettability when neutralized. Therefore, the differences on the charged surfaces result from the surface charges only. On positively charged surfaces, the  $\cos(\theta)$  is slightly higher, namely, the water contact angle is slightly lower. The  $\cos(\theta)$  slightly increases as the positive charge density increases. On negatively charged surfaces, the  $\cos(\theta)$  is almost insensitive to the charge density. The maximum difference of  $\cos(\theta)$  on positively and nega-

tively charged surfaces is about 0.05 at final temperature of 70 °C. Overall, the surface charges up to 0.1 C/m<sup>2</sup> nominally affect the wettability of pure water comparing to the same uncharged surface. The increasing tendency of  $\cos(\theta)$  on charged surfaces agrees with the understanding of surface wetting. Stronger interaction between water droplet and the solid surface induces lower WCA or higher  $\cos(\theta)$ . When the surface is charged, the Coulomb attraction enhances the strength of the water–substrate interaction, thus decreases WCA.<sup>[8]</sup> Microscopically, when the surface is charged, the polarization of water molecules in the bottom layer turns to the direction normal to the surface, contributing more opportunities for hydrogen bonds to be formed with the upper water molecules.<sup>[9]</sup> Interaction of water with positively charged surface is 36% stronger than that with negatively charged one with the same charge density of 0.6 C/m<sup>2</sup>, according to molecular dynamic simulations.<sup>[8]</sup>

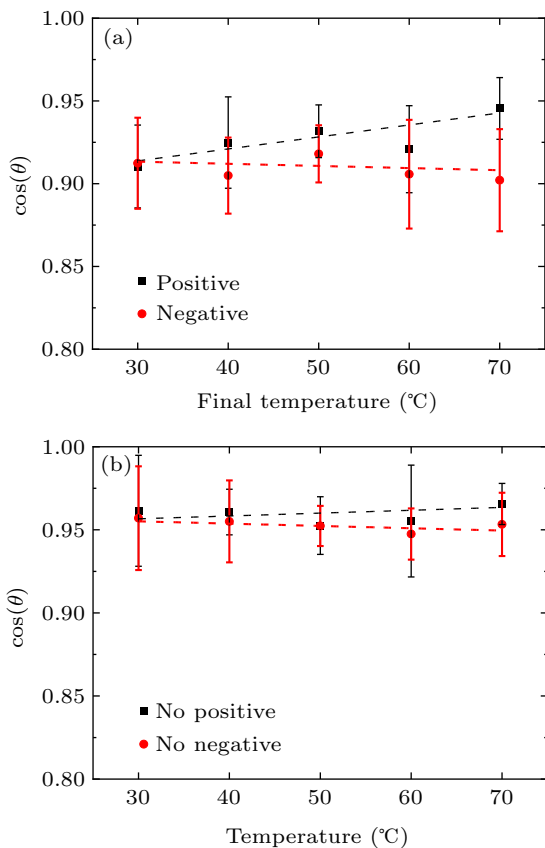


**Fig. 3.** Cosine of contact angle of water droplets on LiTaO<sub>3</sub> crystals at various temperatures. (a) The  $\cos(\theta)$  on charged crystals heated from room temperature to various final temperatures. (b) The  $\cos(\theta)$  on crystals without net charge.

## 5. Effect of environmental aerosols

In environmental aerosols, surface charges participate in the adsorption of contaminations in aerosols. The adsorption can influence the WCA values since they greatly contribute to the chemical properties of surfaces. Here we explore how surface charges influence WCA in aerosols.

### 5.1. Water contact angle in aerosols

We observe that  $\cos(\theta)$  hardly decreases on neutralized surface during the first 60 minutes in the aerosol (Fig. 4(a)). The controlled aerosol is sufficiently clean to maintain the surface tension of the neutralized surface for an hour since the outside air is effectively diluted by high purity nitrogen in the chamber. Benefitting from the clean aerosol in which WCA maintains almost constant on neutralized surfaces, the change in evolution of WCA in the presence of surface charges can directly reflect the role of surface charges. If the surface is heated to 30 °C,  $\cos(\theta)$  gradually decreases in 60 minutes (Fig. 4(b)). If the crystal is treated by UVO for 5 minutes before 20 or 40 minutes,  $\cos(\theta)$  increases immediately and gradually decreases afterward in the aerosol. UVO is the combination of ultraviolet and ozone, which can decompose organic contaminations and clean surfaces. The aerosol has the opposite influence onto the wettability of the surface comparing to UVO treatment. If the crystal is put into saturated organic vapor of 1-octadecene without surface charges for 50 minutes and then treated by UVO for 5 minutes, the  $\cos(\theta)$  increases upon UVO treatments (Fig. 4(c)). Therefore, we conclude that adsorption of organic contaminations in the aerosol decreases  $\cos(\theta)$ .<sup>[14–18]</sup> There are complex chemical compositions in particulate matters in the air of Beijing, which contains considerable proportion of organic matters including alkanes, olefins and alkynes.<sup>[23,24]</sup> These contribute to contaminations in the aerosol. Figure 4(d) shows the x-ray photoelectron spectroscopy (XPS) spectrum of carbon 1X peak of crystals in the controlled aerosol for 0 minutes, 1 minute and 120 hours, where the difference between 1 min (light red) or 120 h (light blue) and 0 min in the inset shows more organic contaminations for longer aerosol exposure. Furthermore, the energy dispersive spectrometer (EDS) detection shows that the atomic concentrations of carbon on crystals in the controlled aerosol for 1 minute and 120 hours are  $2.12 \pm 0.36\%$  and  $9.06 \pm 0.23\%$ , respectively. The amount of adsorbed organic contaminations gradually increases in the aerosol, resulting in the decrease of surface tension and the decrease of  $\cos(\theta)$ .

### 5.2. Effect of charged surfaces and electrification in aerosols

In the environmental aerosol, whether the surface is neutral or charged leads to different evolution of  $\cos(\theta)$ , as the comparison between Figs. 4(a) and 4(b). We modify the surface charge density by heating crystals from room temperature to 30 °C, 50 °C or 70 °C and detect the evolution of  $\cos(\theta)$  every quarter for 60 minutes (Fig. 5). The controlled aerosols are all the same except that the pipe in which high purity nitrogen flows into the chamber (see methods) is straight brass pipe, straight teflon pipe or bent teflon pipe. We detect each combined situation of charge densities and controlled aerosols with different pipes. The fitted curves are linear for straight pipes and exponential for bent pipes.

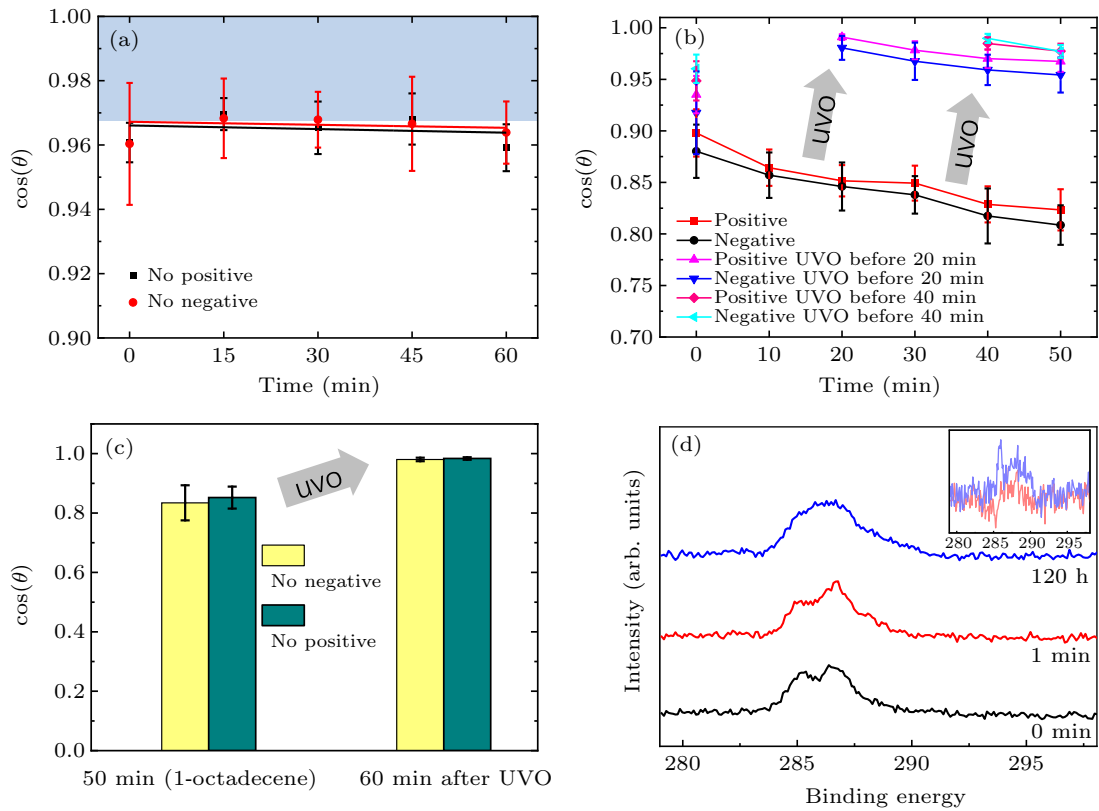


**Fig. 4.** (a) Evolution of  $\cos(\theta)$  of water droplets on neutralized  $\text{LiTaO}_3$  crystals for 60 minutes in the controlled aerosol. The rectangle shows that  $\cos(\theta)$  hardly decreases. (b) Evolutions of  $\cos(\theta)$  of water droplets on  $\text{LiTaO}_3$  crystals heated to  $30^\circ\text{C}$  in the controlled aerosol for 50 minutes and those be treated by UVO for 5 minutes before 20 or 40 minutes. (c) The  $\cos(\theta)$  of water droplets on  $\text{LiTaO}_3$  crystals in saturated vapor of 1-octadecene at room temperature for 50 minutes and 60 minutes after being treated by UVO for 5 minutes. (d) XPS spectrum of carbon 1X peak of  $\text{LiTaO}_3$  in the controlled aerosol for 0 minutes (black), 1 minute (red) or 120 hours (blue). The inset is the difference between 1 min (light red) or 120 h (light blue) and 0 min.

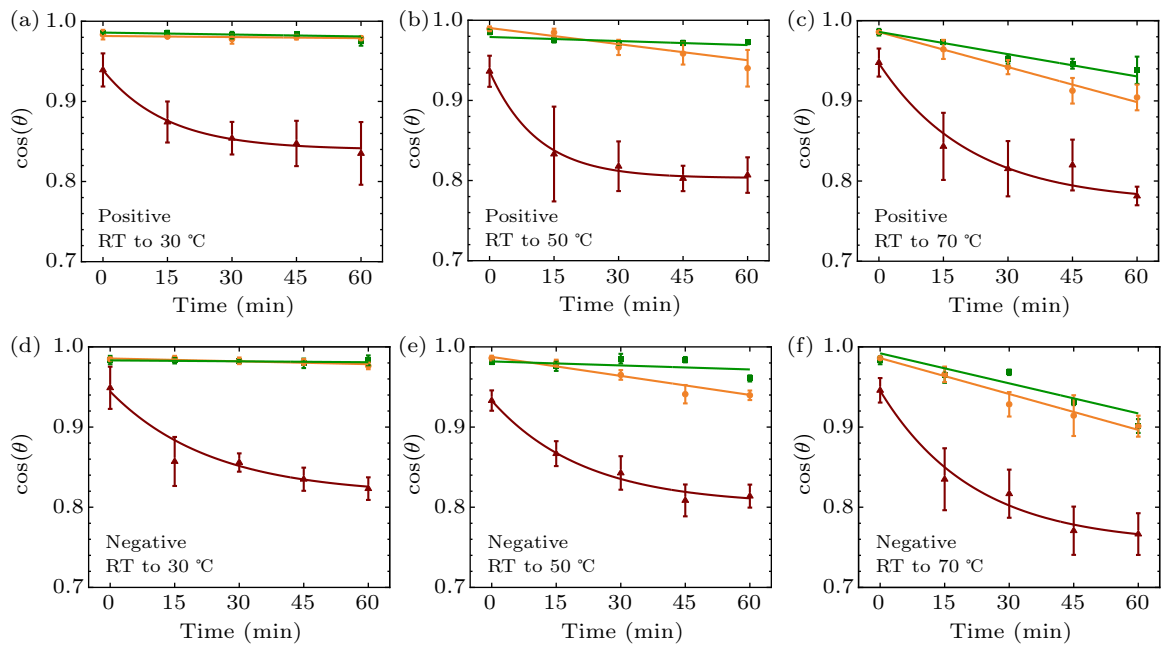


**Fig. 5.** Evolution of  $\cos(\theta)$  of water droplets on  $\text{LiTaO}_3$  crystals heated to various temperatures in various aerosols. The pipe from which high purity nitrogen flows into the chamber is straight brass (green), straight teflon (orange) or bent teflon (brown).

The value of  $\cos(\theta)$  gradually decreases for each case due to the adsorption of contaminations in aerosols. The decreasing rate on more highly charged surface is higher. There is no distinction between positive or negative surface charges.

For comparison among aerosols with different pipes, the decrease of  $\cos(\theta)$  is higher for straight teflon than for straight brass, and the cases with bent teflon pipes are the highest. For easy viewing, we calculate the decreases from 0 to 60 minutes



and list them in Tables 1 and 2.

Higher density of surface charges indicates a stronger Coulomb attraction between the crystal surface and contaminations in the aerosols, which enhances the amount of adsorbed contaminations, resulting in the higher decrease of  $\cos(\theta)$ . Contaminations in aerosols can be charged when passing through the pipes due to friction. They are both positively and negatively charged with various compositions according to the triboelectric series,<sup>[25,26]</sup> thus the adsorption is of no difference on positively or negatively charge surfaces. For straight pipes of the same length, the amount of charged molecules in aerosols through metallic brass is less than that in insulating teflon.<sup>[25,26]</sup> The bent teflon pipe is longer and bent, generating more charges in aerosols.<sup>[26–28]</sup> The more charged are the aerosols, the more organic contaminants can be adsorbed on the crystal surface, leading to lower  $\cos(\theta)$ . Here the surface charges and charged aerosols decrease the  $\cos(\theta)$  via enhancing the adsorption of organic contaminants.

**Table 1.** Decrease of  $\cos(\theta)$  from 0 to 60 minutes on positively charged surface.

Final temperature	Straight brass	Straight teflon	Bent teflon
30 °C	0.01091	0.00438	0.10417
50 °C	0.01325	0.0492	0.12955
70 °C	0.04745	0.0816	0.16636

**Table 2.** Decrease of  $\cos(\theta)$  from 0 to 60 minutes on negatively charged surface.

Final temperature	Straight brass	Straight teflon	Bent teflon
30 °C	0.00035	0.00858	0.12577
50 °C	0.01995	0.0464	0.1192
70 °C	0.08179	0.08491	0.17927

## 6. Conclusion and perspectives

In summary, by employing LiTaO<sub>3</sub> crystal, we obtain controllable surface charges and explore their effects on the contact angle of pure water. We find that the net surface charges up to 0.1 C/m<sup>2</sup> can nominally affect the wettability comparing to the neutral cases, by imposing stronger interactions between the surfaces and water molecules in a few interfacial water layers. However, in aerosol environment, even a small amount of surface charge can efficiently increase the water contact angle. This decrease of surface tension roots from the adsorption of organic contaminants with the help of Coulomb attraction between the charged surfaces and the contaminants. Our results provide a fundamental understanding of interactions between surface charges and water in various environments. We expect that these findings are helpful for developing new ways for the electric control of wetting and microfluidics in real aerosol environments.

## Acknowledgements

Project supported by the National Natural Science Foundation of China (Grant Nos. 12025407, 11934003, 91850120, and 11774328), the Key R&D Program of China (Grant No. 2016YFA0300902), and the Chinese Academy of Sciences.

## References

- [1] Ehre D, Lavert E, Lahav M and Lubomirsky I 2010 *Science* **80** 672
- [2] Eral H B, Augustine D M, Duits M H G and Mugele F 2011 *Soft Matter* **7** 4954
- [3] Wang C L, Yang H J, Wang X, Qi C H, Qu M Y, Sheng N, Wan R Z, Tu Y S and Shi G S 2020 *Commun. Chem.* **3** 27
- [4] Mugele F and Baret J C 2005 *J. Phys. Condens. Matter* **17** R705
- [5] Zhao Y P and Wang Y 2013 *Rev. Adhes. Adhes.* **1** 114
- [6] Manukyan G, Oh J M, Van Den Ende D, Lammertink R G H and Mugele F 2011 *Phys. Rev. Lett.* **106** 014501
- [7] Giovambattista N, Rossky P J and Debenedetti P G 2012 *Annu. Rev. Phys. Chem.* **63** 179
- [8] Wang W D, Zhang H Y, Li S and Zhan Y J 2016 *Nanotechnology* **27** 075707
- [9] Giovambattista N, Debenedetti P G, Rossky P J 2007 *J. Phys. Chem. B* **111** 9581
- [10] Wang C L, Zhou B, Tu Y S, Duan M Y, Xiu P, Li J Y and Fang H P 2012 *Sci. Rep.* **2** 358
- [11] Qi C H, Zhou B, Wang C L, Zheng Y J and Fang H P 2017 *Phys. Chem. Chem. Phys.* **19** 6665
- [12] Quéré D 2008 *Annu. Rev. Mater. Res.* **38** 71
- [13] Glass A M 1968 *Phys. Rev.* **172** 564
- [14] Kùlah E, Marot L, Steiner R, Romanyuk A, Jung T A, Wàckerlin A and Meyer E 2017 *Sci. Rep.* **7** 43369
- [15] Li Z, Wang Y, Kozbial A, Shenoy G, Zhou F, McGinley R, Ireland R, Morganstein B, Kunkel A, Surwade S P, Li L and Liu H T 2013 *Nat. Mater.* **12** 925
- [16] Kozbial A, Gong X, Liu H and Li L 2015 *Langmuir* **31** 8429
- [17] Kozbial A, Li Z, Conaway C, Conaway C, McGinley R, Dhingra S, Vahdat V, Zhou F, D'Urso B, Liu H T and Li L 2014 *Langmuir* **30** 8598
- [18] Aria A I, Kidambi P R, Weatherup R S, Xiao L, Williams J A and Hofmann S 2016 *J. Phys. Chem. C* **120** 2215
- [19] Lang F L, Yan W Q, Zhang Q and Cao J 2013 *China Environmental Science* **33** 1153 (in Chinese)
- [20] Fan X Y, Wen T X, Xu Z J and Wang Y S 2013 *Environmental Chemistry* **32** 742 (in Chinese)
- [21] Brownridge J D 1992 *Nature* **358** 287
- [22] Hòlscher R, Schmidt W G and Sanna S 2014 *J. Phys. Chem. C* **118** 10213
- [23] Lv Z, Han L H, Cheng S Y and Yang X W 2018 *Journal of Beijing University of Technology* **44** 463 (in Chinese)
- [24] Zhang H L, Wu Z H, Li B, Liu K K, Yue T T and Zhang Y J 2020 *Research of Environmental Sciences* **33** 526 (in Chinese)
- [25] Williams M W 1976 *J. Macromol. Sci. Part C* **14** 251
- [26] Masuda H, Komatsu T, Mitsui N and Iinoya K 1977 *J. Electrostat.* **2** 341
- [27] Cole B N, Baum M R and Mobbs F R 1969 *Proc. Instr. Mech. Engrs.* **184** 77
- [28] Xu C, Zhang B B, Wang A C, Zou H Y, Liu G L, Ding W B, Wu C S, Ma M, Feng P Z, Lin Z Q and Wang Z L 2019 *ACS Nano* **13** 2034